UILU-ENG-91-2012

# CIVIL ENGINEERING STUDIES

STRUCTURAL RESEARCH SERIES NO. 564

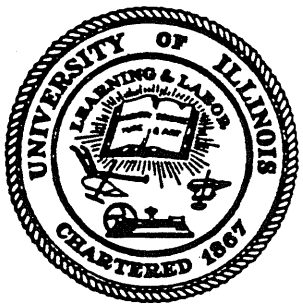


ISSN: 0069-4274

# EXPERIMENTAL *J* ESTIMATION FORMULAS FOR SINGLE EDGE NOTCH BEND SPECIMENS CONTAINING MISMATCHED WELDS

By
MARK T. KIRK
ROBERT H. DODDS, JR.

A Report on a Research Project
Sponsored by the
DAVID TAYLOR RESEARCH CENTER
METALS AND WELDING DIVISION
ANNAPOLIS, MARYLAND

DEPARTMENT OF CIVIL ENGINEERING
UNIVERSITY OF ILLINOIS AT
URBANA-CHAMPAIGN
URBANA, ILLINOIS
DECEMBER 1991

# Experimental *J* Estimation Formulas for Single Edge Notch Bend Specimens Containing Mismatched Welds

By

Mark T. Kirk
Robert H. Dodds, Jr.
*Department of Civil Engineering*
*University of Illinois*

*A Report on a Research Project Sponsored by the:*

*DAVID TAYLOR RESEARCH CENTER*
*METALS AND WELDING DIVISION*

*Annapolis, Maryland 21402*

University of Illinois
Urbana, Illinois
December 1991

50272-101

| REPORT DOCUMENTATION PAGE | 1. REPORT NO. UILU-ENG-91-2012 | 2. | 3. Recipient's Accession No. |
|---|---|---|---|

**4. Title and Subtitle**
**Experimental *J* Estimation Formulas for Single Edge Notch Bend Specimens Containing Mismatched Welds**

5. Report Date: December 1991
6.

**7. Author(s)**
Mark T. Kirk and Robert H. Dodds, Jr.

8. Performing Organization Report No.: SRS 564

**9. Performing Organization Name and Address**
University of Illinois at Urbana-Champaign
Department of Civil Engineering
205 N. Mathews Avenue
Urbana, Illinois 61801

10. Project/Task/Work Unit No.

11. Contract(C) or Grant(G) No.: N61533-90-K-0059

**12. Sponsoring Organization Name and Address**
David Taylor Research Center
Metal and Welding Division, Code 281
Annapolis, Maryland 21402

13. Type of Report & Period Covered: Interim: 1-1-91 to 11-30-91
14.

15. Supplementary Notes

**16. Abstract (Limit: 200 words)**

This study addresses the effect of weld strength mismatch on *J* estimation formulas for single edge notch bend, SE(B), specimens. A crack located on the weld joint centerline is treated. The combined effects of weld groove type, degree of mismatch, and crack depth to specimen width ($a/W$) ratio are considered by performing plane-strain elastic-plastic finite element analyses of SE(B) specimens containing a variety of common weld groove details. This study reveals that treating a welded bend specimen as if it is made entirely from weld metal limits *J* estimation errors. The maximum *J* estimation error observed for +/- 20% mismatch is 15% based on LLD and 10% based on CMOD. The all weld metal approximation fails to properly account for the effect of the weld on the limit load and on plasticity distribution within the SE(B) specimen. However, these two inadequacies produce errors of opposite sign. This error cancellation helps promote accurate *J* estimation.

**17. Document Analysis** a. Descriptors

Weldments, Mismatch Effects, *J* Estimation, Fracture Mechanics, Finite Elements

b. Identifiers/Open-Ended Terms

c. COSATI Field/Group

| 18. Availability Statement | 19. Security Class (This Report) | 21. No. of Pages |
|---|---|---|
| Release Unlimited | UNCLASSIFIED | 17 |
| | 20. Security Class (This Page) UNCLASSIFIED | 22. Price |

(See ANSI-Z39.18)

OPTIONAL FORM 272 (4-77)
Department of Commerce

# ABSTRACT

This study addresses the effect of weld strength mismatch on $J$ estimation formulas for single edge notch bend, SE(B), specimens. A crack located on the weld joint centerline is treated. The combined effects of weld groove type, degree of mismatch, and crack depth to specimen width ($a/W$) ratio are considered by performing plane-strain elastic-plastic finite element analyses of SE(B) specimens containing a variety of common weld groove details. This study reveals that treating a welded bend specimen as if it is made entirely from weld metal limits $J$ estimation errors. The maximum $J$ estimation error observed for +/- 20% mismatch is 15% based on LLD and 10% based on CMOD. The all weld metal approximation fails to properly account for the effect of the weld on the limit load and on plasticity distribution within the SE(B) specimen. However, these two inadequacies produce errors of opposite sign. This error cancellation helps promote accurate $J$ estimation.

# ACKNOWLEDGMENTS

The authors are pleased to recognize the many helpful discussions with J.J. DeLoach, R. Gordon, M.G. Vassilaros, and T.W. Montemarano. This report was prepared as part of the Surface Ship and Submarine Materials Block under the sponsorship of I. L. Caplan (David Taylor Research Center, Code 011.5). The work of the first author was performed in the Civil Engineering Department at the University of Illinois as part of an extended term training program. The work supports DTRC Program Element 62234N, Task Area RS345S50.

Computational support and reproduction of this report were made possible by the David Taylor Research Center, Contract No. N61533-90-K-0059 to the University of Illinois.

# TABLE OF CONTENTS


| Section No. | | Page |
|---|---|---|
| **1.** | **Introduction** | 1 |
| **2.** | ***J* Estimation Formulas** | 1 |
| **3.** | **Approach** | 2 |
| **4.** | **Finite Element Modelling** | 3 |
| **5.** | **Results and Discussion** | 5 |
| | 5.1 *J* Estimation for Unwelded (Homogeneous) Specimens | 5 |
| | 5.2 Finite Element Results for +/− 20% Matching | 6 |
| | 5.3 Justification of Assumptions in Approach | 12 |
| | 5.3.1 *J*−Integral Path Independence | 12 |
| | 5.3.2 HAZ Modelling | 13 |
| | 5.3.3 Effect of Constitutive Properties | 14 |
| | 5.3.4 Effect of Extreme Overmatch | 15 |
| **6.** | **Summary and Conclusions** | 15 |
| **7.** | **References** | 17 |

# LIST OF TABLES


| Table No. | | Page |
|---|---|---|
| 1 | Constitutive properties for weldment analysis. | 3 |
| 2 | $\eta_{pl}$ values for $a/W = 0.15$ SE(B) specimens. | 12 |
| 3 | Constitutive properties for weldment analysis. | 15 |

# LIST OF FIGURES


| Figure No. | | Page |
|---|---|---|
| 1 | Weldment geometries analyzed. | 2 |
| 2 | Finite element model of a SE(B) specimens containing an $a/W = 0.15$ crack in a single bevel joint. | 4 |
| 3 | Errors associated with $J$ estimates for homogeneous SE(B) specimens using Sumpter's $\eta$. | 6 |
| 4 | Comparison of $\eta$ values reported by Sumpter (with those calculated by finite element analysis for $n = 13$. | 6 |
| 5 | Errors associated with $J$ estimates for homogeneous SE(B) specimens using finite element $\eta$ values. | 7 |
| 6 | $J$ estimation errors for welded SE(B) specimens. | 8 |
| 7 | Variation of plastic work with $J_{pl}$ for an $a/W = 0.15$ crack in a 45° single-V weld. | 7 |
| 8 | Plastic zone shape for homogeneous SE(B) loaded to $J = 1100$ lbs/in overlaid on two weld joints. | 9 |
| 9 | Effect of minimum distance to the weld / plate interface on $J$ estimation error at $J = 1000$ lbs/in. | 9 |
| 10 | Effects of changing joint width on $\eta_{pl}$ for mismatched weldments. | 10 |
| 11 | Possible interactions between plasticity and limit load effects on $\eta_{pl}$ for an overmatched weldment. | 11 |
| 12 | Effect of $L_{min}$ on $J$ estimation error at $J = 1000$ lbs/in and on $\eta_{pl}$ for an $a/W = 0.15$ crack in a square groove weld. | 11 |
| 13 | Comparison of $J$ estimation errors at $J = 1000$ lbs/in for square groove weldments with errors for other groove types. | 12 |
| 14 | Variation of $J$ with domain (path) radius for an $a/W = 0.15$ crack in a 20% undermatched 60° double-V weld groove. | 12 |
| 15 | Variation of $J$ with domain radius for an uncracked 10% undermatched 45° single-V weld. 'X' mark on inset plot indicates applied loading when $J$ evaluated. | 13 |
| 16 | Finite element mesh detail and yield properties for square groove HAZ model. | 14 |
| 17 | $J$ estimation errors for detailed HAZ model compared to $J$ estimation errors for bi-material model. | 14 |
| 18 | Effect of constitutive properties on $J$ estimation errors. | 15 |
| 19 | Effect of extreme mismatch on $J$ estimation errors. | 16 |
| 20 | Effect of extreme mismatch on variation of plastic work - $J_{pl}$ proportionality. | 16 |

## 1. INTRODUCTION

Fracture toughness testing of weldments raises many complications not encountered with testing of homogeneous materials. The special procedures needed to prepare specimens for testing and to perform post-test certification of the sampled microstructure have been widely researched and described in the literature [1-3]. However, relatively little information is available regarding the effect of weld strength and strain hardening inhomogeneity on the relation of experimentally measured quantities (i.e. load line displacement (LLD), crack mouth opening displacement (CMOD), and load) to fracture toughness parameters ($J$). Both Cray et al. [4] and Dong and Gordon [5] reported significant effects of weld strength mismatch on these relationships for double-V and square groove welds, respectively. Sumpter [6] proposed experimental $J$ estimation formulas which, while explicitly accounting only for crack depth effects, were demonstrated to predict $J$ values within 18% of a finite element solution for double-V weldments [7]. However, the applicability of these formulas to the wide range of weld groove types encountered in practice (e.g. single bevel, single-V, J-groove, double bevel, double-U) has not been demonstrated. Further, it would be useful to assess the relative benefits of $J$ estimates based on LLD vs. $J$ estimates based on CMOD.

This study addresses the effect of weld strength mismatch on $J$ estimation formulas for single edge notch bend, SE(B), specimens. A crack located in the weld metal on the weldment centerline is treated in detail. This study considers the combined effects of weld groove type, degree of mismatch, and crack depth to specimen width ($a/W$) ratio.

## 2. J ESTIMATION FORMULAS

When testing SE(B) specimens, values of applied load, LLD, and CMOD are monitored and used to estimate the applied $J$ by one of the following formulas [6]

$$J = \frac{K^2(1-\nu^2)}{E} + \frac{\eta_{pl}}{Bb} A_{pl}|_{LLD} \tag{2.1}$$

$$J = \frac{K^2(1-\nu^2)}{E} + \frac{\eta_{pl}}{Bb} A_{pl}|_{CMOD} \left( \frac{S}{4(a + r_p b)} \right) \tag{2.2}$$

where $K$ is the linear elastic stress intensity factor, $\nu$ is Poisson's ratio, $E$ is Young's modulus, $B$ is the specimen thickness, $a$ is the initial crack length, $b$ is the initial remaining ligament, $A_{pl}|_{LLD}$ is the area under the load - plastic LLD curve, $A_{pl}|_{CMOD}$ is the area under the load - plastic CMOD curve, and $S$ is the bend span. The symbols $\eta_{pl}$ and $r_{pl}$ denote the plastic eta factor and the plastic rotation factor, respectively. Currently, ASTM Standards address only deeply cracked specimens ($a/W > 0.45$) for which $\eta_{pl} = 2$ and $r_{pl} = 0.44$ [8-9]. However, to closely match service conditions, shallow crack ($a/W < 0.25$) fracture toughness specimens are often tested. Sumpter [6] determined the following dependency of $\eta_{pl}$ and $r_{pl}$ on $a/W$ by limit load analysis of the SE(B) specimen:

| for $a/W < 0.282$ | for $a/W > 0.282$ |
|---|---|
| $\eta_{pl} = 0.32 + 12\frac{a}{W} - 49.5\left(\frac{a}{W}\right)^2 + 99.8\left(\frac{a}{W}\right)^3$ | $\eta_{pl} = 2.0$ |

(2.3)

| for $a/W < 0.3$ | for $a/W > 0.3$ |
|---|---|
| $r_{pl} = 0.3 + 0.5\frac{a}{W}$ | $r_{pl} = 0.45$ |

(2.4)

Equation (2.2) can be expressed in an alternative form, consistent with eqn. (2.1), i.e.

$$J = \frac{K^2(1-\nu^2)}{E} + \frac{\eta_{pl}|_{CMOD}}{Bb} A_{pl}|_{CMOD} \tag{2.5}$$

where

$$\eta_{pl}|_{CMOD} = \eta_{pl} \frac{S}{4(a + r_p b)} \tag{2.6}$$

For standard specimens, $S = 4W$, so eqn. (2.6) simplifies to

$$\eta_{pl}|_{CMOD} = \frac{\eta_{pl}}{a/W + r(1-a/W)} \tag{2.7}$$

Combining eqn. (2.7) with eqns. (2.3) and (2.4) gives

for $a/W < 0.282$

$$\eta_{pl}|_{CMOD} = \frac{0.32 + 12\frac{a}{W} - 49.5\left(\frac{a}{W}\right)^2 + 99.8\left(\frac{a}{W}\right)^3}{0.3 + 1.2\frac{a}{W} - 0.5\left(\frac{a}{W}\right)^2} \tag{2.8}$$

for $a/W > 0.282$

$$\eta_{pl}|_{CMOD} = \frac{2}{0.3 + 1.2\frac{a}{W} - 0.5\left(\frac{a}{W}\right)^2}$$

for $a/W < 0.3$

$$\eta_{pl}|_{CMOD} = \frac{2}{0.45 + 0.55\frac{a}{W}}$$

In this investigation, $J$ is estimated from LLD using eqns. (2.1) and (2.3) and from CMOD using eqns. (2.5) and (2.8).

## 3. APPROACH

Currently, $J$ and $CTOD$ estimation for SE(B) specimens, monolithic or welded, can be based only on the formulas summarized in Section 2. In this study, plane-strain elastic-plastic finite element analyses of SE(B) specimens containing a variety of common weld groove details (i.e. single-V, double-V, square groove, single bevel) are performed. The variation of CMOD and LLD with applied load quantified by these analyses permit evaluation of $\eta_{pl}$ and $\eta_{pl}|_{CMOD}$. This information establishes a baseline needed to judge the applicability of proposed $J$ estimation formulas to weldments. Further, these finite element data allow development and validation of alternative estimation strategies should those available prove inadequate. The cases illustrated in Figure 1 are each modelled as 20% overmatched, homogeneous (no weld), and 20% undermatched. Unless indicated otherwise, the constitutive properties detailed in Table 1 are used. The weldment is modelled as a bi-material with no transition zone (heat affected zone, or HAZ) placed between the weld and plate properties. The strain

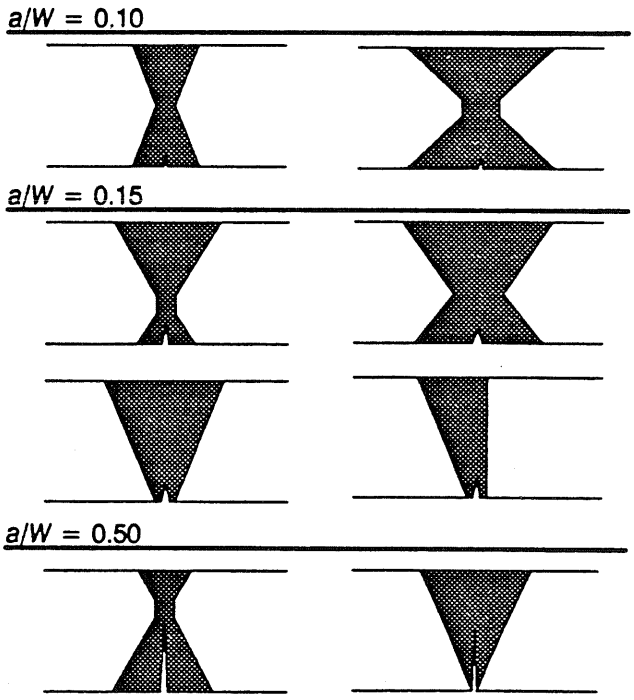


Figure 1: Weldment geometries analyzed.

hardening exponents in Table 1 are calculated from yield stress based on an experimental correlation applicable to construction steels developed by Barsom and Rolfe[10]:

$$n = \left[\frac{\sigma_o}{15}\right]^{\frac{4}{3}} \qquad (\sigma_o \text{ is in ksi}) \tag{3.1}$$

Certain aspects of this approach, adopted for expediency, require justification to ensure the applicability of these results to real weldments. Modelling a weldment as a bi-material raises two issues:

1. The "correct" $J$ from the finite element analysis is ambiguous as path independence is not assured for in-homogeneous bodies.
2. The applicability of these results to real weldments having a constitutive property transient across the HAZ is uncertain.

Further issues raised include

3. The calculation of strain hardening capacity from yield strength using eqn. (3.1), while physically realistic, results in different absolute hardening capacities depending upon the plate yield strength selected for analysis. It is not apparent, for example, that the results of an analysis of a 20% undermatched weld joining 60 ksi yield strength steel (plate $n$ = 6.3, weld $n$ = 4.7) apply to a 20% undermatched weld joining 100 ksi yield strength steel (plate $n$ = 12.5, weld $n$ = 9.3).
4. Quite large amounts of overmatch can occur in practice (e.g. welding A36 steel with an E8018 electrode producing approximately 50% overmatch) which lie outside the main focus of this study.

This investigation addresses each of these four issues.

Table 1: Constitutive properties for weldment analyses

| % Mismatch | Weld | | Plate | |
|---|---|---|---|---|
| | $\sigma_o$ [ksi] | $n$ | $\sigma_o$ [ksi] | $n$ |
| 20% Over | 104 | 13 | 86 | 10 |
| No Weld | — | — | 104 | 13 |
| 20% Under | 104 | 13 | 130 | 18 |

Yield strength ($\sigma_o$) and strain hardening exponent ($n$) are coefficients in the Ramberg-Osgood constitutive relation:

$$\frac{\epsilon}{\epsilon_o} = \frac{\sigma}{\sigma_o} + a\left(\frac{\sigma}{\sigma_o}\right)^n$$

where $a = 1$ and $\epsilon_o = E/\sigma_o$

## 4. FINITE ELEMENT MODELLING

Two-dimensional, plane-strain finite element analyses of SE(B) specimens are performed using conventional small strain theory. These analyses are conducted using the POLO-FINITE finite element analysis software [12] on an engineering workstation.

Uniaxial stress-strain behavior is described using the Ramberg-Osgood model

$$\frac{\epsilon}{\epsilon_o} = \frac{\sigma}{\sigma_o} + a\left(\frac{\sigma}{\sigma_o}\right)^n \tag{4.1}$$

where $\sigma_o$ is the reference (0.2% offset yield) stress, $\epsilon_o = \sigma_o/E$ is the reference strain, $\alpha$ is a dimensionless parameter, and $n$ is the strain hardening coefficient.

$J_2$ deformation plasticity theory (i.e. nonlinear elasticity) describes the multi-axial material model. Total strains and total stresses are related by

$$\frac{\epsilon_{ij}}{\epsilon_o} = \alpha\frac{3}{2}\left(\frac{\sigma_e}{\sigma_o}\right)^{n-1}\frac{s_{ij}}{\sigma_o}, \qquad \sigma_e = \sqrt{\frac{3}{2}s_{ij}s_{ij}} \tag{4.2}$$

where $s_{ij}$ is the stress deviator and $\sigma_e$ is the Mises equivalent tensile stress. The total strain, $\epsilon_{ij}$, is partitioned into deviatoric and volumetric terms that vary with stress according to

$$\epsilon_{ij} = \left[\frac{1+\nu}{E} + \frac{3\alpha\epsilon_o}{2\sigma_o}\left(\frac{\sigma_e}{\sigma_o}\right)^{n-1}\right]s_{ij} + \frac{1-2\nu}{3E}\sigma_{kk}\delta_{ij} \tag{4.3}$$

where $\sigma_{kk}$ is the trace of the stress tensor and $\delta_{ij}$ is the Kronecker delta.

Finite element models are constructed for each combination of $a/W$ ratio and weld joint geometry. These computations apply to SE(B) specimens of standard proportions; the unsupported span is four times the specimen width. Models of symmetric joints contain approximately 900 elements and 2850 nodes, while the non-symmetric mesh of the single bevel weld contains 1414 elements and 4431 nodes. Figure 2 illustrates this model. Eight noded, plane-strain isoparametric quadrilateral elements are used throughout. Reduced (2 x 2) Gaussian integration is used to eliminate locking of arbitrarily shaped elements. A half-circular core of elements surrounds the crack tip in all models. This core consists of eight equally sized wedges, 22.5° each, of elements in the $\theta$ direction. Each wedge contains 30 quadrilateral elements whose radial dimension decreases geometrically with decreasing element distance to the crack tip. The eight crack tip elements are collapsed into wedges with the initially coincident nodes left unconstrained to permit development of crack tip blunting deformations. The side nodes of these elements are retained at the mid-point position. This modelling produces a $1/r$ strain singularity[1], appropriate in the limit of perfect plasticity. Crack tip element size ranges from 0.2% to 0.02% of the crack depth depending on the crack depth modelled.

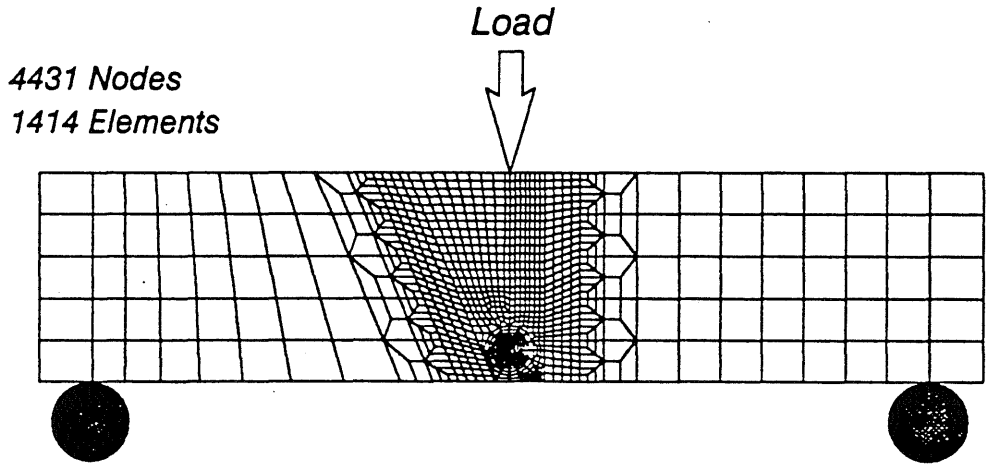


Figure 2: Finite element model of a SE(B) specimen containing an $a/W$ = 0.15 crack in a single bevel joint.

1. $r$ is distance from the crack tip.

Load is uniformly distributed over two small elements and applied at the center of the compression face of the specimen to eliminate the local singularity effects caused by a concentrated nodal load. Between 30 and 50 variably sized load steps are taken to deform the specimen until the *CTOD* is 5% of the crack length. Strict criteria at each step ensure convergence of calculated stresses and strains to the third significant figure. Two to three full Newton iterations at each load step are generally required to satisfy this criteria. As deformation plasticity is strain path independent, converged solutions are load step size invariant.

The *J*-integral is computed at each load step using a domain integral method [13,14]. *J* values calculated over domains adjacent to and remote from the crack tip, but not crossing a bi-material interface, are within 0.003% of each other, as expected for deformation plasticity combined with these detailed meshes. *CTOD* is estimated from the blunted shape of the crack flanks using the Rice 45° intercept procedure. LLD is taken as the relative displacement in the loading direction of a node on the symmetry plane located approximately $0.4b$ in front of the crack tip and of a node located a distance $W/2$ above the support. This procedure eliminates the effect of locally high displacements in the vicinity of both the load and support points on the LLD. The $\eta_{pl}$ factor is determined from these results by calculating the slope of $J_{pl}$ ($J_{pl} = J_{total} - K^2(1-\nu^2)/E$) vs. $A_{pl}|_{LLD}$ at each load step. This slope typically shows very little variation after the first few load steps, these being predominantly elastic and thus not expected to provide reliable $\eta_{pl}$ factors. These initial values are disregarded. The factor $\eta_{pl}|_{CMOD}$ is determined similarly using $A_{pl}|_{CMOD}$.

## 5. RESULTS AND DISCUSSION

### *5.1 J Estimation for Unwelded (Homogeneous) Specimens*

Prior to investigating the accuracy of eqns. (2.1) and (2.5) applied to welded SE(B) specimens, the accuracy of these estimation formulas for homogeneous test pieces is assessed. Finite element analyses are used to determine the variation of *J* with load and displacement for $a/W$ values between 0.1 and 0.5. A *J* estimation error is calculated for each load step as follows:

$$\%Error = \frac{J_{FE} - J_{EST}}{J_{FE}} \cdot 100 \qquad (5.1.1)$$

where $J_{FE}$ is the *J* value calculated for a weldment by the domain integral technique and $J_{EST}$ is the *J* value calculated from the load – displacement curve using either eqn. (2.1) or (2.5) and an $\eta$ value from eqn. (2.3) or (2.8), respectively. These errors, while quite small at $a/W = 0.5$, approach a constant value at large deformations of approximately 10% for the two shallow cracks modelled, as illustrated in Figure 3. Compared to the scatter typical of cleavage fracture toughness ($J_c$) data [15], an error of 10% is insignificant. However, the development of a range of conditions needing no mismatch correction would greatly simplify fracture toughness testing of weldments. It seems therefore prudent to use the most accurate *J* estimation strategy practicable. To this end, these finite element results for homogeneous specimens are used to quantify the variation of both $\eta_{pl}$ and $\eta_{pl}|_{CMOD}$ with $a/W$ for a material with a Ramberg-Osgood strain hardening coefficient of 13. These $\eta$ values differ from those reported by Sumpter, as shown in Figure 4. The data in Figure 5 demonstrate that use of the finite element $\eta$ values improve *J* estimation accuracy. Further, use of these $\eta$ values indicates the better accuracy of CMOD based *J* estimates, eqn. (2.5), than of LLD based *J* estimates, eqn. (2.1), an advantage not apparent in Figure 3. Despite this better accuracy, experimental complexities associated with CMOD measurement for shallow cracks

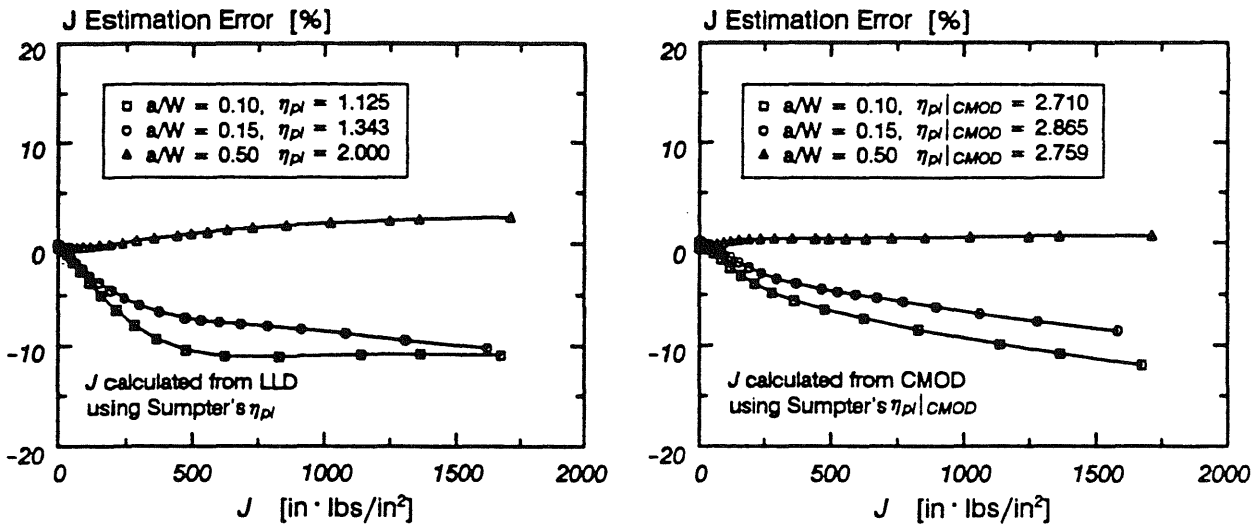


Figure 3: Errors associated with $J$ estimates for homogeneous SE(B) specimens using Sumpter's $\eta$

may necessitate use of LLD based $J$ estimates. Therefore, both estimation strategies are investigated for weldments.

### 5.2 *Finite Element Results for + /- 20% Matching*

The $J$ estimation error which results from the approximation of a welded SE(B) specimen as a SE(B) specimen made entirely of weld metal are summarized in Figure 6 (page 8). These, and all subsequent, $J$ estimates are calculated using $\eta$ values determined by finite element analysis. While both eqn. (2.1) and (2.5) are quite accurate, generally having below 10% error, $J$ estimation from CMOD is consistently more accurate than $J$ estimation from LLD. Previous investigators have qualitatively argued the superiority of CMOD based estimates. Dawes contends that, for highly overmatched welds, plastic deformation of the lower strength plate remote from the

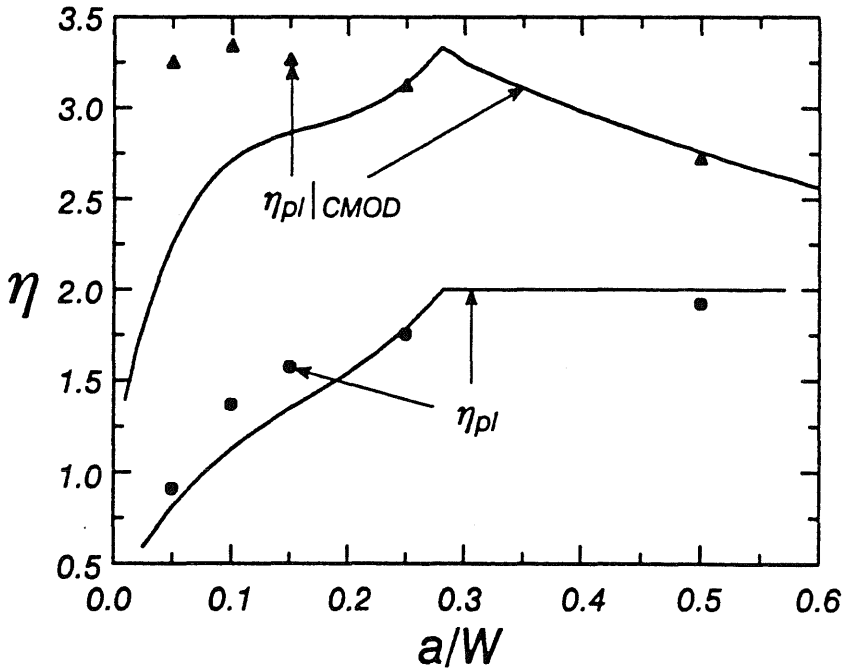


Figure 4: Comparison of $\eta$ values reported by Sumpter (lines) with those calculated by finite element analysis (symbols) for $n = 13$.

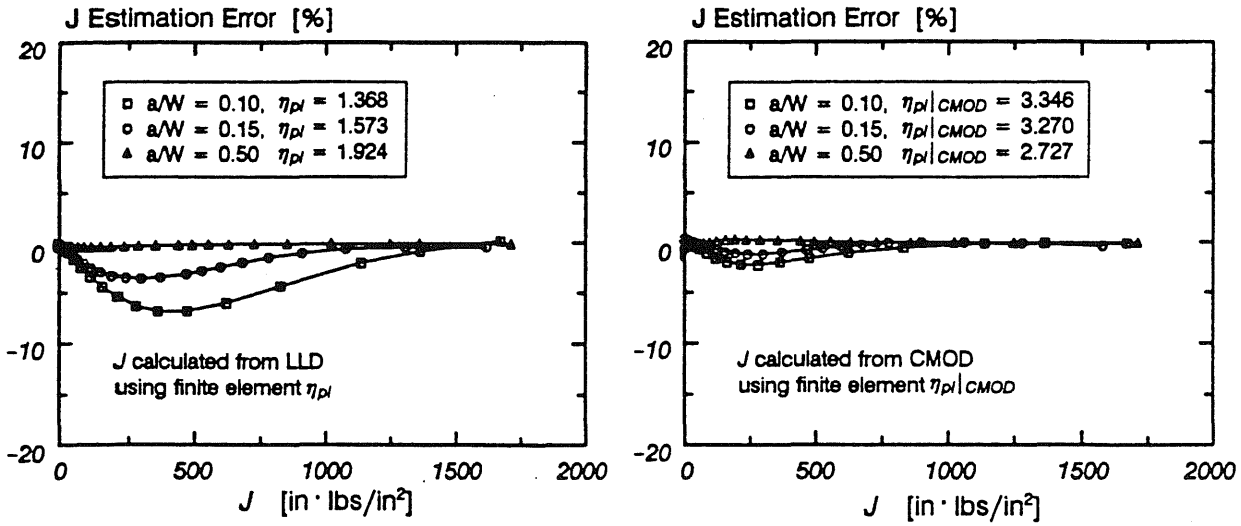


Figure 5: Errors associated with $J$ estimates for homogeneous SE(B) specimens using finite element $\eta$ values.

crack can completely dissipate the applied plastic work [16]. In this situation, the weld deposit "rides along" on the deformation of the plate, causing $A_{pl}|_{LLD}$ to increase while both $A_{pl}|_{CMOD}$ and $J_{pl}$ saturate. This is not the case for these weldments, as shown in Figure 7. CMOD based $J$ estimates are more accurate as a consequence of the better accuracy of eqn. (2.5) for homogeneous specimens.

Comparison of the errors in Figure 6 indicates that $J$ estimates for deeply cracked weldments are much more accurate than for shallow cracks. Deep cracks confine plastic flow to the net section. Thus, a mismatch effect in a deeply cracked bar occurs only if a significant portion of the material ahead of the crack is not made of weld metal. Shallow cracked SE(B) specimens experience gross section yielding (GSY) which stresses significant portions of both the plate and the weld metal beyond yield. The accuracy of the all weld metal approximation de-

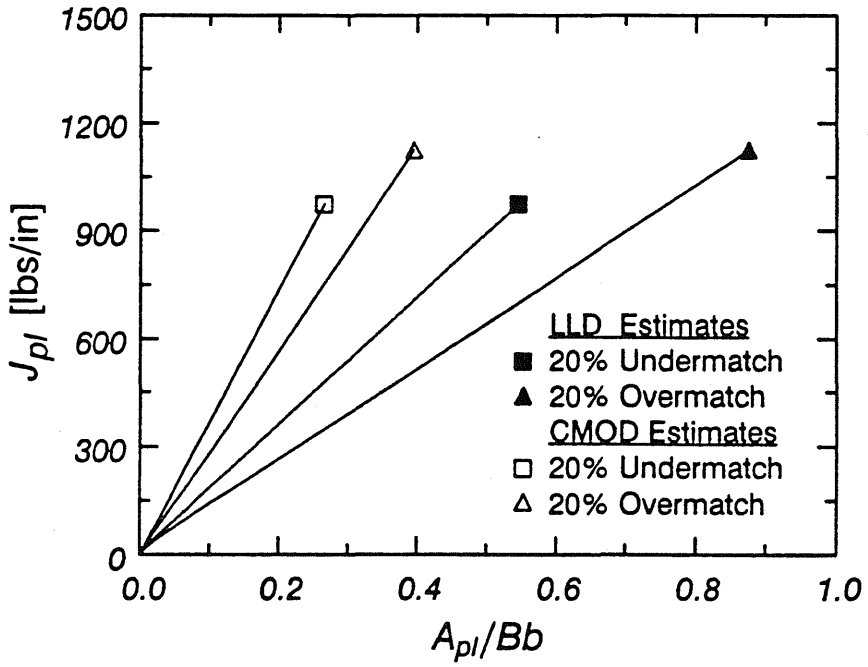


Figure 7: Variation of plastic work with $J_{pl}$ for an $a/W=0.15$ crack in a 45° single-V weld.

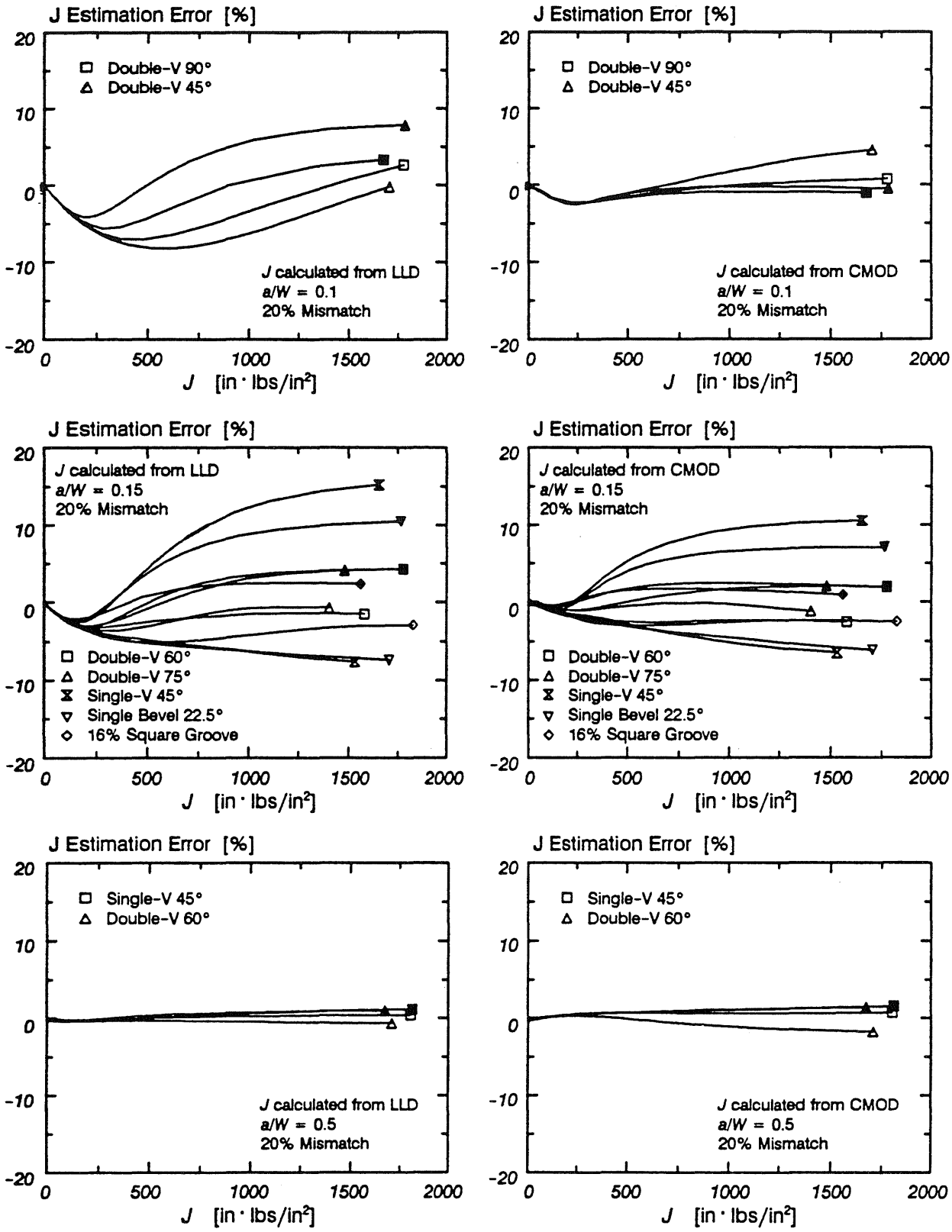


Figure 6: $J$ estimation errors for welded SE(B) specimens (solid symbols for overmatch, open symbols for undermatch). Relative crack sizes are $a/W = 0.1$ (top), $a/W = 0.15$ (middle), and $a/W = 0.5$ (bottom).

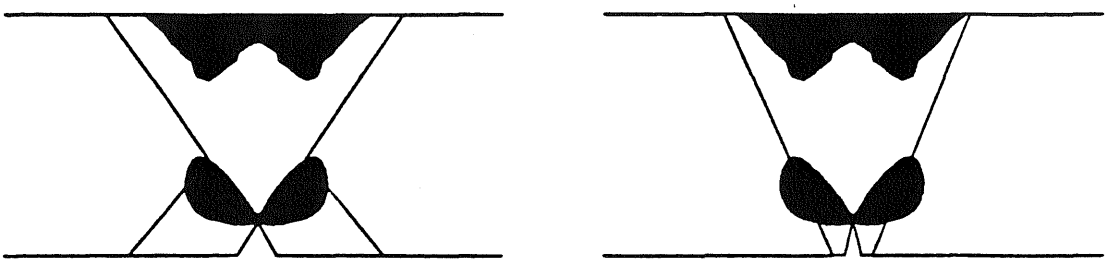

Figure 8: Plastic zone shape for homogeneous SE(B) loaded to $J = 1150$ lbs/in overlaid on two weld joints

pends on the shape of the weld joint relative to the shape of the GSY plastic zone. In Figure 8, the plastic zone shape for a homogeneous SE(B) specimen with $a/W = 0.15$ is overlaid on two of the weld groove geometries analyzed. The single-V joint splits the plastic zone between plate and weld metal more evenly than the double-V joint, for which the plastic zone lies almost entirely within the weld metal. On this basis, greater $J$ estimation errors are expected for the single-V weld than for the double-V weld, as shown in Figure 6. The data in Figure 6 further indicate that $J$ estimates for undermatched welds are generally more accurate than for overmatched welds. Undermatch localizes post yield deformation into the weld metal, thereby improving the accuracy of the all weld metal approximation. Conversely, overmatching spreads plasticity away from the weldment into the surrounding plate, making the all weld metal approximation less accurate.

Beyond these general conclusions, the features of a weld joint / crack geometry combination that maximize or minimize mismatch effects remain elusive. The minimum distance from the crack tip to the weld / plate interface ($L_{min}$) is expected to play an important role. However, the data presented in Figure 9 for $a/W = 0.15$ specimens fail to show any systematic trend[2]. For a fixed weld groove geometry, the variation of $L_{min}$ (joint size) affects

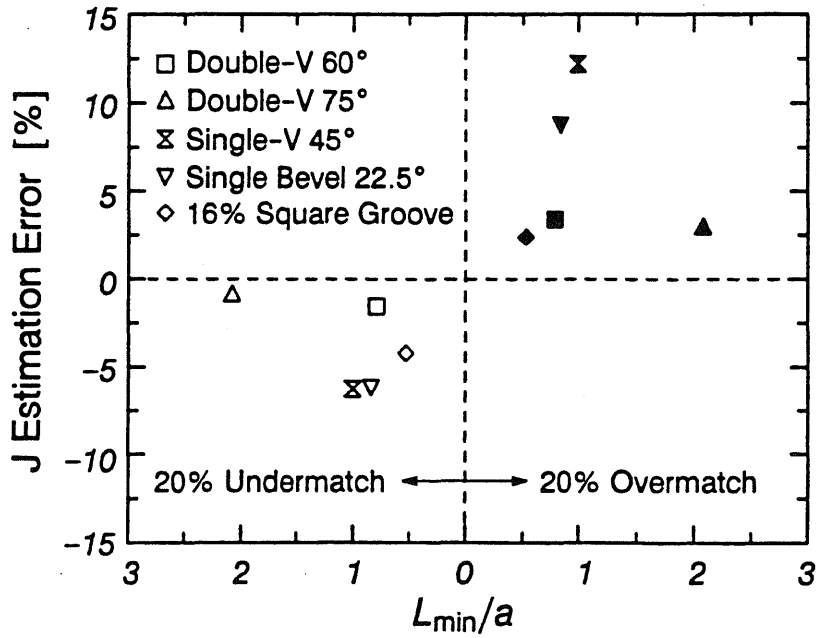


Figure 9: Effect of minimum distance to the weld plate interface on LLD based $J$ estimation error at $J$ = 1000 lbs/in (solid symbols for overmatch, open symbols for undermatch).

2. Only LLD based $J$ estimates are addressed in the remainder of Section 5.2. Similar trends to those discussed are seen for CMOD based $J$ estimates.

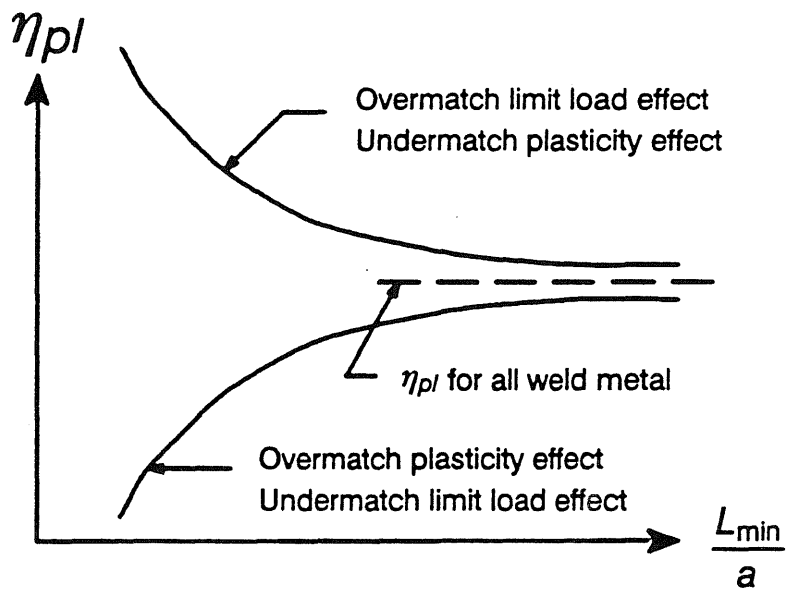


Figure 10: Effects of changing joint width on $\eta_{pl}$ for mismatched weldments.

both the limit capacity and the plasticity distribution within the specimen. These effects change $\eta_{pl}$ in opposite ways, as illustrated in Figure 10 and detailed in the following:

*For Overmatch:*

1. Limit Load Reducing joint width ($L_{min}/a$ decreasing), drops the limit load as the high strength weld decreases in size. This reduces plastic work (area under the load – plastic displacement curve) but has little effect on $J_{pl}$, causing $\eta_{pl}$ to increase.
2. Plasticity Transfer into Plate Reducing joint width increases the area of the plate remote from the crack tip that becomes plastic. The plate would remain elastic were the weld absent, thus plasticity transfer increases plastic work. However, $J$ is unaffected as this deformation is non-singular. Therefore, $\eta_{pl}$ decreases with decreasing joint width.

*For Undermatch:*

1. Limit Load Reducing joint width ($L_{min}/a$ decreasing), elevates the limit load as the low strength weld decreases size. This increases plastic work but has little effect on $J_{pl}$, causing $\eta_{pl}$ to decrease.
2. Plasticity Concentrated in Weld Reducing joint width concentrates plasticity into the lower strength weld metal, thereby reducing the volume of plastically deformed material. This reduces plastic work. However, $J$ is unaffected as this deformation is non-singular. Therefore, $\eta_{pl}$ increases with reducing joint width.

As indicated in Figure 10, when the joint becomes large both the limit load and the plasticity effect become small and $\eta_{pl}$ approaches the value for a SE(B) made entirely of weld metal. As the joint becomes thin, $\eta_{pl}$ must approach the value for a SE(B) made entirely of the plate (ignoring interface effects). $\eta_{pl}$ values for all plate and all weld metal SE(B) specimens were calculated from finite element results and are summarized in Table 2. These values are fairly close together, so neither the plasticity effect or the limit load effect can dominate over the entire range of weld joint size. An interaction must occur, as depicted schematically in Figure 11.

To quantify the effect of crack tip proximity to the weld/plate interface, a parametric study is performed for a square groove weld in which the groove width is systematically varied. These results, presented in Figure 12, show that $\eta_{pl}$ varies between the all weld metal and all plate limits. For both overmatching and undermatching,

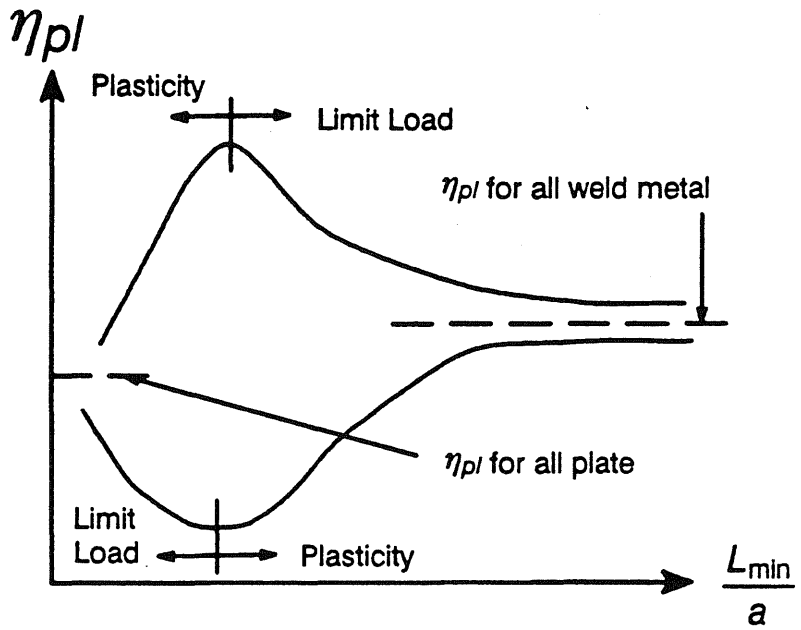


Figure 11: Possible interactions between plasticity and limit load effects on $\eta_{pl}$ for an overmatched weldment.

plasticity effects dominate when the interface is far from the crack tip, while limit load effects dominate for narrower joints. As these errors have opposite effects on $\eta_{pl}$, their interaction helps keep $J$ estimation errors small.

In Figure 13, the variation of $J$ estimation error for the $a/W = 0.15$ square grooved specimen is superimposed with the errors determined for more commonly used weld joints. The error for the square groove specimen partitions the more complex joints into two sets: those with greater errors (single-V and single bevel) and those with lesser errors (double-V). This seems to indicate that the combined plasticity and limit load effects are, at this crack depth, more significant for the single-V / single bevel joints and less severe for the double-V joints. A more quantitative explanation of the cause of this phenomena is the subject of on-going research.

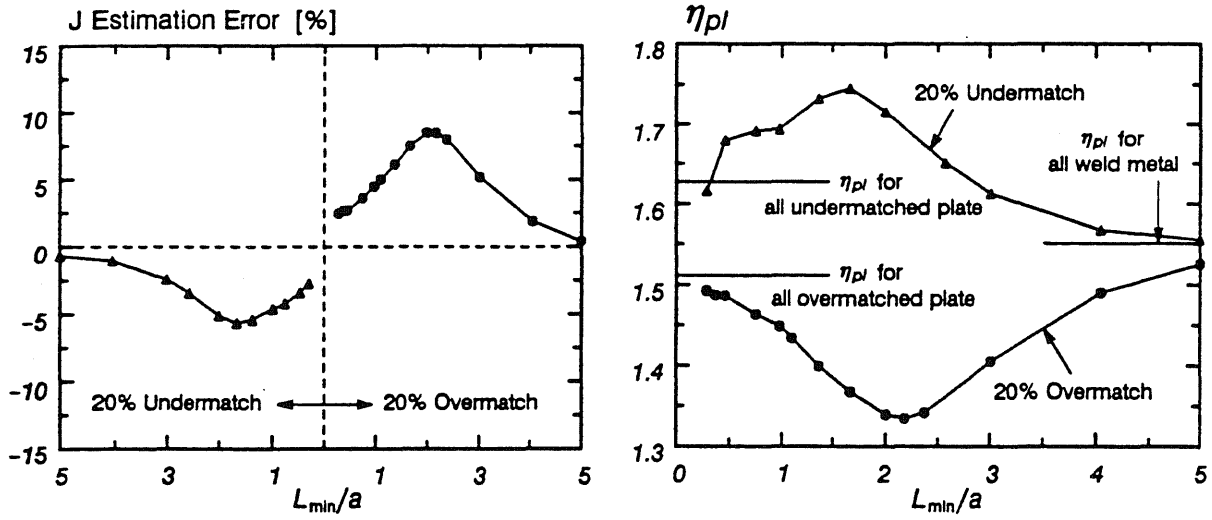


Figure 12: Effect of $L_{min}$ on $J$ estimation error at $J = 1000$ lbs/in and on $\eta_{pl}$ for an $a/W = 0.15$ crack in a square groove weld.

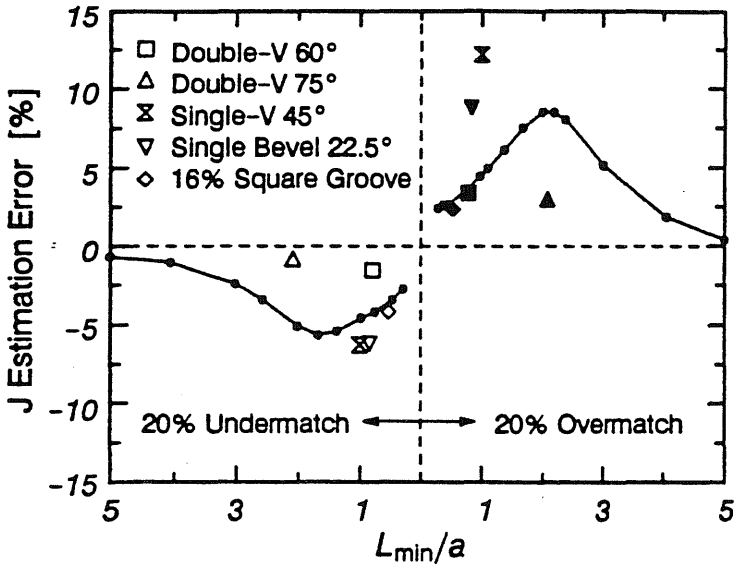


Figure 13: Comparison of $J$ estimation errors at $J = 1000$ lbs/in for square groove weldments (line) with errors for other groove types (solid symbols for overmatch, open symbols for undermatch).

Table 2: $\eta_{pl}$ values for $a/W = 0.15$ SE(B) specimens

| | Strain Hardening Coefficient ($n$) | $\eta_{pl}$ |
|---|---|---|
| Overmatched Plate | 10 | 1.51 |
| Weld Metal | 13 | 1.55 |
| Undermatched Plate | 18 | 1.62 |

### *5.3 Justification of Assumptions in Approach*

#### *5.3.1 J-Integral Path Independence*

The $J$-contour integral proposed by Rice [17] is path independent if the body containing the crack is completely homogeneous, or if the inhomogeneity occurs parallel to the crack [5]. Only the square groove weld in this study meets this requirement. The variation of $J$ with domain (path) radius for an $a/W = 0.15$ crack in a 20% undermatched 60° Double-V weld groove is depicted in Figure 14. At low loads the material along the interface responds elastically. As the elastic modulus of the plate and the weld are identical, no path dependence occurs

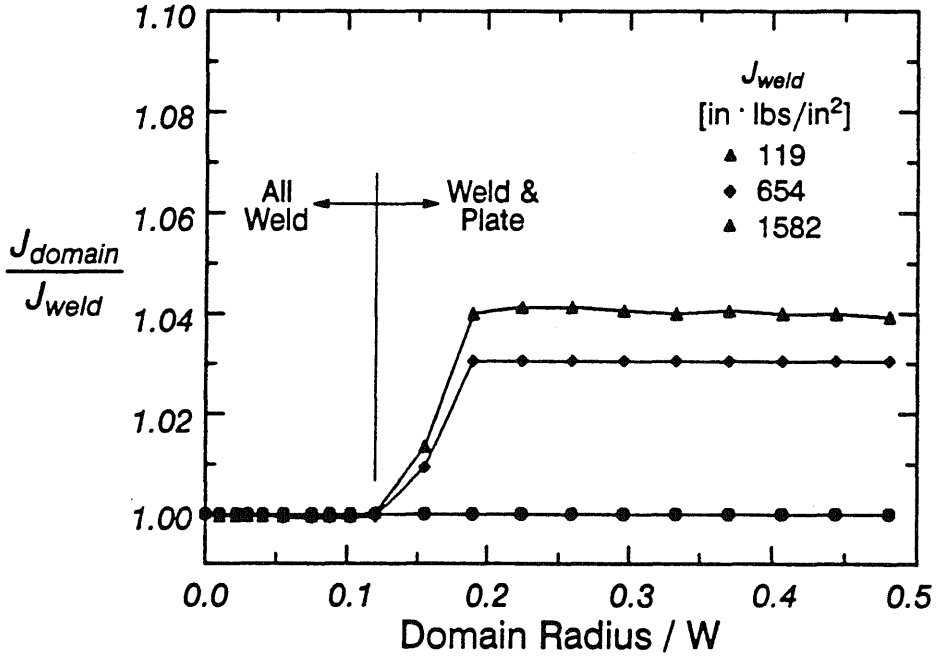


Figure 14: Variation of $J$ with domain (path) radius for an $a/W = 0.15$ crack in a 20% undermatched 60° double-V weld.

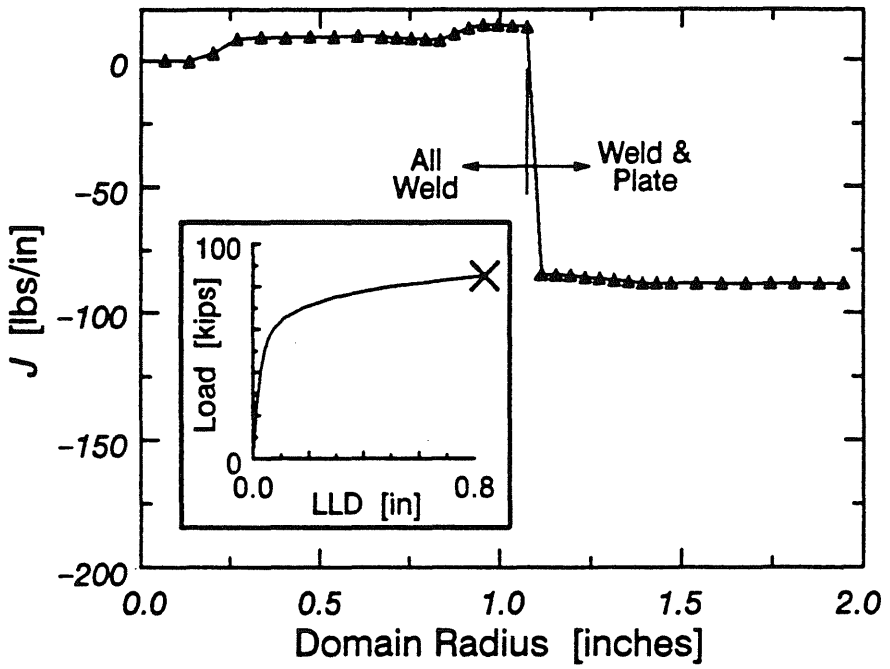


Figure 15: Variation of $J$ with domain radius for an uncracked 10% undermatched 45° single-V weld. 'X' mark on inset plot indicates applied loading when $J$ evaluated.

under these conditions. However, displacement derivatives can be discontinuous across the interface once yielding occurs due to the differing post-yield flow response of the plate and the weld metal. The domain integration to calculate $J$ senses these discontinuities as singularities which, for the 20% undermatched 60° Double-V weldment, increase the $J$ value above the value due to the crack alone. While this is not a large effect, the correct $J$, near tip or far field, is ambiguous (this weldment exhibits the largest path dependency of any considered in this investigation). Further, for weldments where the crack tip and the interface are in closer proximity or for greater degrees of mismatch, path dependencies should be greater and be significant at lower applied loads. To resolve this uncertainty, a finite element analysis was conducted of an uncracked single-V weldment loaded in three point bending. In this analysis, $J$ is zero as there is no crack. Domain integration was performed about a point at the intersection of the neutral axis and the symmetry plane as if a crack tip were there. The variation of $J$ with domain radius from this analysis, shown in Figure 15, clearly indicates that the correct $J$ for a mismatched weldment is determined by integration over a region completely within the weld metal.

### *5.3.2 HAZ Modelling*

The results presented in the preceding sections are determined using finite element models which do not account for the transition in constitutive properties between the weld and the plate. The HAZ is so remote from a crack on the weld centerline and is so thin that it should have little effect on either $J$ or on the ability of the specimen to dissipate plastic work. To demonstrate the validity of ignoring the HAZ, an analysis of a shallow cracked square groove weldment including a highly refined HAZ model was performed. A detail of this model near the crack is shown along with the constitutive properties modelled in Figure 16. The yield strength of the 0.005-inch wide HAZ layer immediately adjacent to the weld is 180 ksi, characteristic of the as-quenched martensite found in the grain coarsened HAZ. Between this high hardness layer and the plate, the HAZ is modelled as seven discrete layers of increasing width and decreasing strength. These models realistically represent both the peak hardness and total HAZ width. Further, this model presents a greater challenge for accurate $J$ estimation errors than oc-

curs in an actual weldment. An actual multi-pass weldment has a discontinuous high strength layer due to re-tempering from multiple passes, rather than the continuous high strength layer modelled here. The $J$ estimation errors produced by these models are compared to those characteristic of the same specimen when modelled as a bi-material, as done in the rest of this study in Figure 17. These data show virtually no effect of HAZ modelling on CMOD based $J$ estimation, and only a slight effect on LLD based $J$ estimation. Thus, the simpler bi-material models used in this investigation appear capable of providing quite accurate estimates of $J$ estimation error for real weldments having a constitutive property gradient across the HAZ.

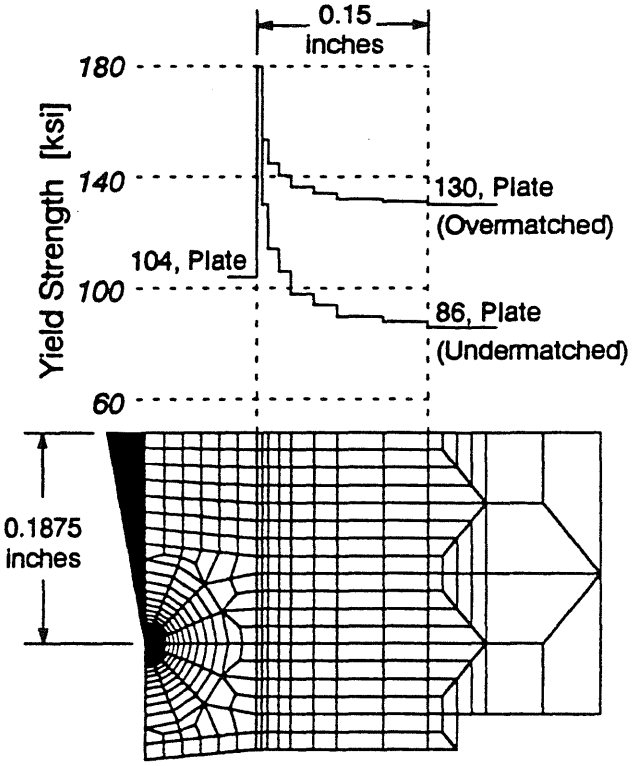


Figure 16: Finite element mesh detail and yield properties for square groove HAZ model.

### 5.3.3 *Effect of Constitutive Properties*

All of the results discussed thus far are generated using one set of constitutive properties. To assess the applicability of these results to mismatch for different constitutive properties, the weldment showing the greatest effect of mismatch (45°Single-V, $a/W = 0.15$) was re-analyzed using properties characteristic of a lower strength steel, given in Table 3. The effect of this change in constitutive properties is illustrated in Figure 18. The error reaches a maximum in both analyses shortly after the plastic part of $J$ exceeds the elastic part, which occurs at a lower applied $J$ in the lower strength material. The inaccuracy in the $J$ estimation schemes is all in the plastic part due to the approximation of $\eta_{pl}$ for the weldment by $\eta_{pl}$ from an all weld metal analysis. Thus, once $J_{pl}$ becomes large compared to $J_{el}$ ($J_{pl}/J_{el} \gg 1$), the maximum error is achieved. This maximum error is only slightly affected by the difference in strain hardening exponent between the two analyses. In summary, the com-

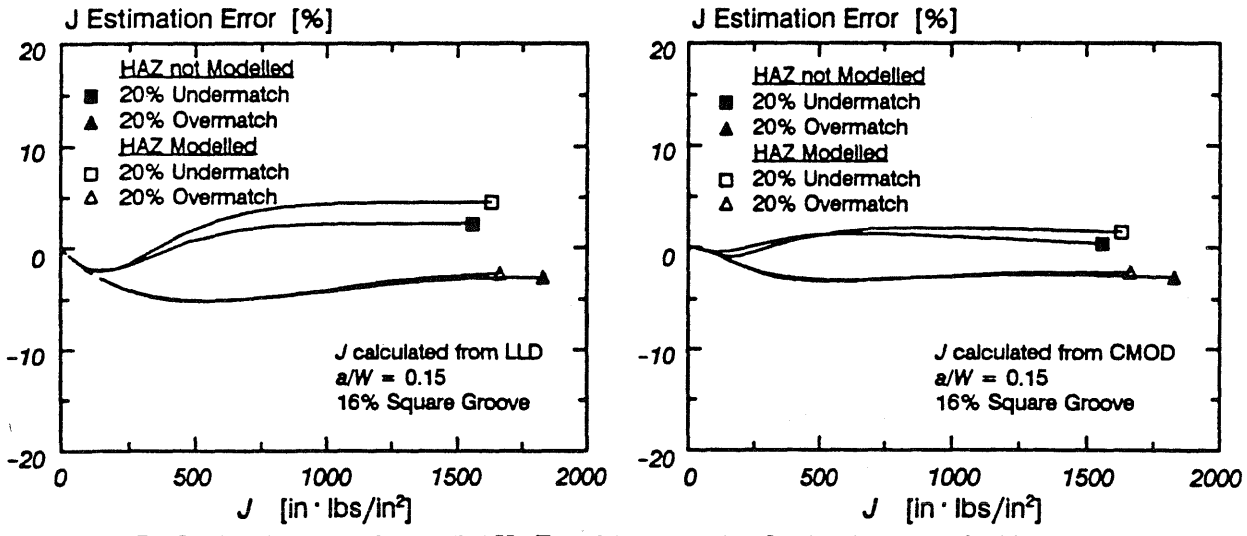


Figure 17: $J$ estimation errors for detailed HAZ model compared to $J$ estimation errors for bi-material model.

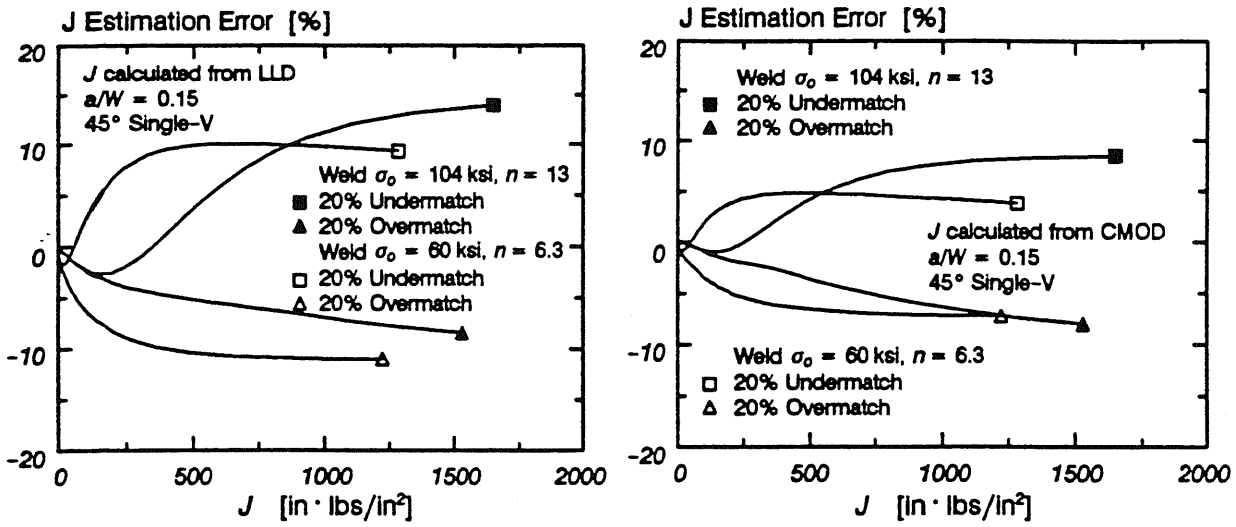


Figure 18: Effect of constitutive properties on $J$ estimation errors.

bined effects of changing either $\sigma_o$ or $n$ produce only second order changes in the maximum $J$ estimation error produced by a given weld groove geometry / crack depth / mismatch combination. Thus, the effect of 20% mismatch on $J$ estimation accuracy in large scale plasticity documented in Figure 18 appears approximately correct irrespective of the baseline $\sigma_o$ and $n$ values used.

Table 3: Constitutive properties for weldment analyses

| % Mismatch | Weld | | Plate | |
|---|---|---|---|---|
| | $\sigma_o$ [ksi] | $n$[1] | $\sigma_o$ [ksi] | $n$[1] |
| 20% Over | 60 | 6.3 | 50 | 5.0 |
| No Weld | — | — | 60 | 6.3 |
| 20% Under | 60 | 6.3 | 75 | 8.5 |

1. $n$ calculated from yield strength by eqn. (3.1)

### *5.3.4 Effect of Extreme Overmatch*

Thus far, all results presented have been for + /- 20% mismatch. However, certain construction practices cause considerably greater overmatch. This is again investigated by performing supplemental analysis of the weldment geometry found most sensitive to mismatch ( 45° Single-V, $a/W = 0.15$). The $J$ estimation errors caused by mismatch ranging from 20% under to 100% over are given in Figure 19. LLD based $J$ estimates become excessive for 50% and 100% mismatch. CMOD based $J$ estimates, while having above 10% error, are considerably more accurate for these highly overmatched cases. As illustrated in Figure 20, CMOD based estimates are more accurate because the proportionality constant between $J_{pl}$ and plastic work based on CMOD ($\eta_{pl}|_{CMOD}$) is changed less by mismatch than is the proportionality constant between $J_{pl}$ and plastic work based on LLD ($\eta_{pl}$). Thus, CMOD based $J$ estimates are clearly preferred for $J$ testing of highly overmatched weldments.

## 6. SUMMARY AND CONCLUSIONS

This study addresses the effect of weld strength mismatch on $J$ estimation formulas for single edge notch bend, SE(B), specimens. A crack located on the weld joint centerline is treated. The combined effects of weld groove type, degree of mismatch, and crack depth to specimen width ($a/W$) ratio are considered by performing plane-

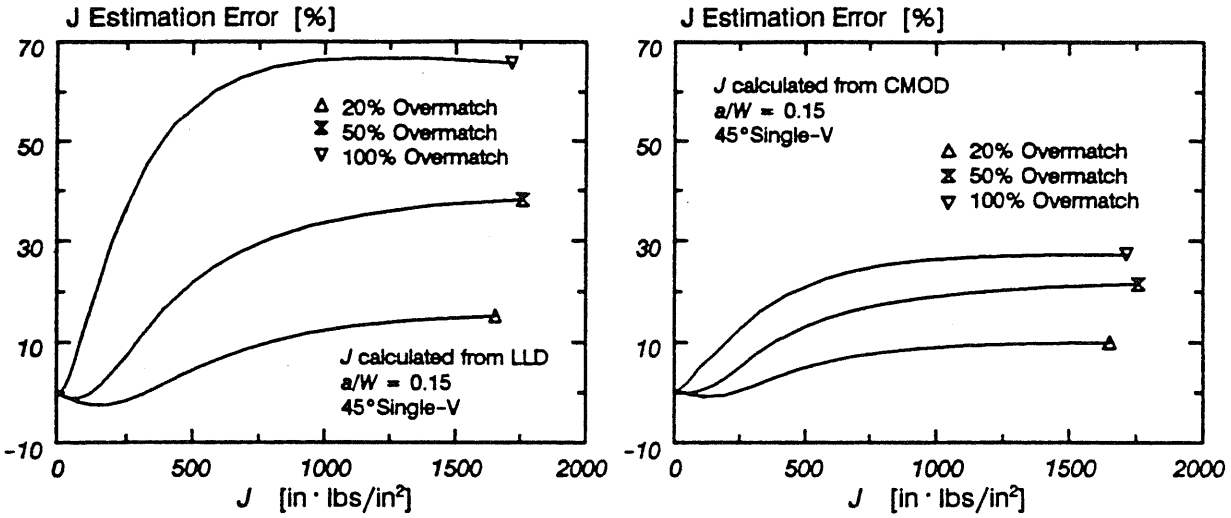


Figure 19: Effect of extreme mismatch on $J$ estimation errors.

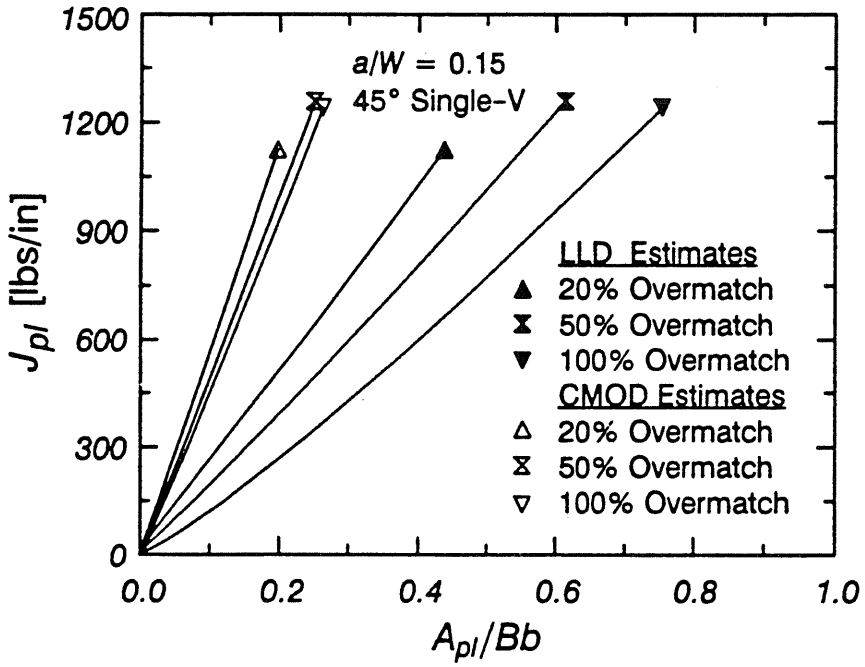


Figure 20: Effect of extreme mismatch on plastic work - $J_{pl}$ proportionality.

strain elastic-plastic finite element analyses of SE(B) specimens containing a variety of common weld groove details. Based on this information, the following conclusions are appropriate:

1. The accuracy of $J$ estimation from either CMOD or LLD is substantially improved by using proportionality constants which relate $J_{pl}$ and plastic work ($\eta$ factors) determined by finite element analysis rather than those based on the limit load analysis suggested by Sumpter. $\eta$ factors for both CMOD and LLD based $J$ estimates are reported herein for a low strain hardening material.
2. For homogeneous materials, improved $J$ estimation accuracy for cracks between 0.1 and 0.5 $a/W$ can be achieved by estimating $J$ from CMOD rather than from LLD.
3. The treatment of a welded bend specimen as if it is made entirely from weld metal limits $J$ estimation errors. The maximum $J$ estimation error observed for +/- 20% mismatch is 15% based on LLD and 10% based on CMOD. The all weld metal approximation fails to properly account for the effect of

the weld on the limit load and on plasticity distribution within the SE(B) specimen. However, these two inadequacies produce errors of opposite sign. This error cancellation helps promote accurate $J$ estimation.

4. The applicable $J$ for a crack located in a mismatched weldment is obtained by calculations over paths / domains located entirely in the weld metal.
5. The constitutive property gradient across the HAZ need not be modelled to accurately assess $J$ estimation errors for cracks located on the weld deposit centerline.
6. CMOD based $J$ estimates are considerably more accurate than LLD based $J$ estimates for cases of extreme overmatch (50% to 100%).

## 7. REFERENCES


[1] Towers, O.L. and Dawes, M.G., "Welding Institute Research on Fatigue Precracking of Fracture Toughness Specimens," *Elastic-Plastic Fracture Test Methods, The User's Experience, ASTM STP 856*, E.T. Wessel and F.J. Loss, Eds., American Society for Testing and Materials, pp. 23–46, 1985.

[2] Dawes, M.G., Squirrell, S.J., and Pisarski, H.G., "$K_{Ic}$, *CTOD*, and $J$ Tests on Weldments," *Nonlinear Fracture Mechanics: Volume II - Elastic-Plastic Fracture, ASTM STP 995*, J.D. Landes, A. Saxena, and J.G. Merkle, eds., American Society for Testing and Materials, pp. 191–213, 1989.

[3] Machida, S., Miyata, T., Toyosada, M., and Hagiware, I., "Study of Methods for *CTOD* Testing of Weldments," *Fatigue and Fracture Testing of Weldments, ASTM STP 1058*, H.I. McHenry and J.M. Porter, Eds., American Society for Testing and Materials, pp. 142–156, 1979.

[4] Cray, M.J., Luxmoore, A.R., and Sumpter, J.D.G., "The Effect of Weld Metal Mismatch on $J$ and *CTOD*," in *Proceedings of the European Symposium on Elastic-Plastic Fracture Mechanics* (to be published), Freiburg, F.R.G., 1989.

[5] Dong, P., and Gordon, J.R., "The Effect of Weld Mismatch on Structural Integrity Assessments," presented at the Sixth Annual North American Welding Research Conference, Columbus, Ohio, November 1990.

[6] Sumpter, J.D.G., "$J_c$ Determination for Shallow Notch Welded Bend Specimens," *Fatigue and Fracture of Engineering Materials and Structures*, Vol. 10, No. 6, pp. 479–493, 1987.

[7] Bleackley, M.H., Jones, R.D., and Luxmoore, A.R., "Path Dependency of the Rice $J$-Integral in Weld Geometries," in *Proceedings of the Sixth European Conference on Fracture: Fracture Control in Engineering Structures*, pp. 643–654, 1986.

[8] ASTM E813-89, Standard test Method for $J_{Ic}$, A Measure of Fracture Toughness.

[9] ASTM E1290-89, Standard test Method for Crack-Tip Opening Displacement (*CTOD*) Fracture Toughness Measurement.

[10] Barsom, J.M., and Rolfe, S.T., *Fracture and Fatigue Control in Structures - Applications of Fracture Mechanics*, p. 265, 1987.

[11] Dodds, R.H., and Lopez, L.A., "Software Virtual Machines for Development of Finite Element Systems," *International Journal for Engineering with Computers*, Vol. 13, pp. 18–26, 1985.

[12] Dodds, R.H., Anderson, T.L., and Kirk, M.T., "A Framework to Correlate a/W Ratio Effects on Elastic-Plastic Fracture Toughness ($J_c$)," *Int J Fract*, Vol. 48, pp. 1–22, 1991.

[13] Li, F.Z., Shih, C.F., and Needleman, A., "A Comparison of Methods for Calculating Energy Release Rates," *Engineering Fracture Mechanics*, Vol. 21, pp. 405–421, 1985.

[14] Shih, C.F., Moran, B., and Nakamura, T., "Energy Release Rate Along a Three-Dimensional Crack Front in a Thermally Stressed Body," *Int J Fract*, Vol. 30, pp. 79–102, 1986.

[15] Sorem, W.A., Dodds, R.H., and Rolfe, S.T., "Effects of Crack Depth on Elastic Plastic Fracture Toughness," *International Journal of Fracture*, Vol. 47, pp. 105–126, 1991.

[16] Dawes, M.G., "Elastic Plastic Fracture Toughness Based on the COD and $J$-Contour Integral Concepts," *Elastic Plastic Fracture, ASTM STP 668*, J.D. Landes, J.A. Begley, and G.A. Clarke, Eds., American Society for Testing and Materials, pp. 307–333, 1979.

[17] Rice, J.R., "A Path Independent Integral and the Approximate Analysis of Strain Concentration by Notches and Cracks," *Journal of Applied Mechanics*, Vol. 35, pp. 379–386, 1968.

# Errata for SRS−564

1. Equation 2.8 on page 2 should read

for $a/W < 0.282$

$$\eta_{pl}|_{CMOD} = \frac{0.32 + 12\frac{a}{W} - 49.5\left(\frac{a}{W}\right)^2 + 99.8\left(\frac{a}{W}\right)^3}{0.3 + 1.2\frac{a}{W} - 0.5\left(\frac{a}{W}\right)^2}$$

for $0.282 < a/W < 0.3$

$$\eta_{pl}|_{CMOD} = \frac{2}{0.3 + 1.2\frac{a}{W} - 0.5\left(\frac{a}{W}\right)^2}$$

for $a/W > 0.3$

$$\eta_{pl}|_{CMOD} = \frac{2}{0.45 + 0.55\frac{a}{W}}$$

2. Figure 16 on page 14 should appear as shown to the right

3. On page 15, the third line should read "... accuracy in large scale plasticity documented in Figure 6."

4. On page 15, the fourth line in Section 5.3.4 should read "... ranging from 20% over to 100% over ..."

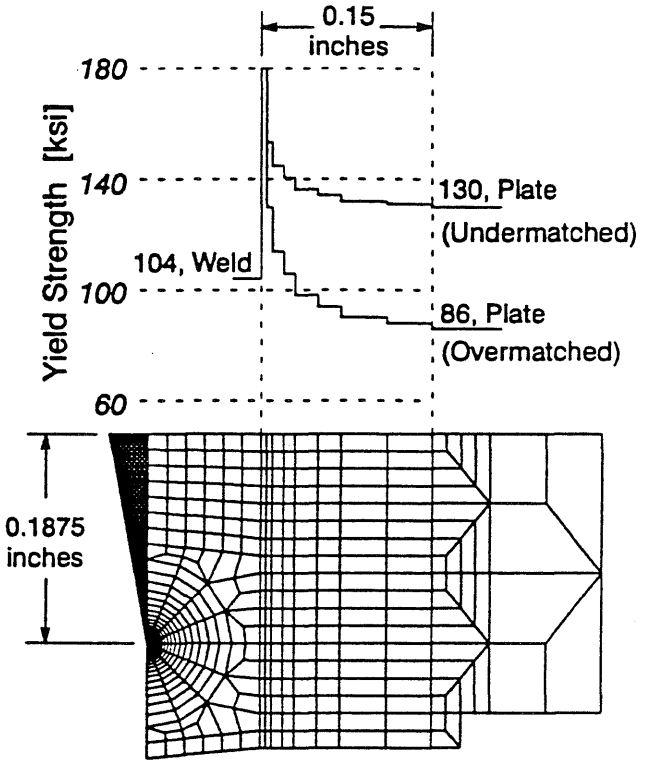


Figure 16: Finite element mesh detail and yield properties for square groove HAZ model. $n$ is calculated from yield strength by eqn. 3.1.